Biomass Conversion and Biorefinery
https://doi.org/10.1007/s13399-023-05175-9

ORIGINAL ARTICLE

Characterization of ex situ developed bacterial cellulose/ZnO-NPs nanocomposite for antimicrobial evaluation

Ahmed K. Saleh[1] · **Ali Hamzah Alessa**[2] · **Awatif M. E. Omran**[3]

Received: 24 October 2023 / Revised: 20 November 2023 / Accepted: 23 November 2023

Abstract
The prevention of various infections in wounds can be achieved through the advancement of antimicrobial materials. Bacterial cellulose (BC) has the ability to carry and convey the nanoparticles to create a wound-healing bandage due to its extensive surface area and numerous pores within the BC membrane structure. Within the scope of this investigation, BC was produced from *Lactiplantibacillus plantarum* AS.6 under static conditions, and the obtained BC hydrogel was adorned with zinc oxide nanoparticles (ZnO-NPs) via an ex situ process for enhancing the antimicrobial efficacy of the produced nanocomposite membrane. The structure and properties of the BC/ZnO-NPs nanocomposite membrane were investigated with X-ray diffraction (XRD), scanning electron microscopy, and TEM. The findings suggested that the act of immersing the BC hydrogel in the synthesized ZnO-NPs resulted in a uniform and even distribution within the BC matrix. In any circumstance, the BC/ZnO-NPs nanocomposite membrane showed excellent antimicrobial properties against all of the models of microbes used, suggesting potential applications as a bactericidal membrane for promoting wound healing activity.

Keywords Bacterial cellulose · Ex situ modification · BC/ZnO-NPs · Antimicrobial activity

1 Introduction

The growing demand for sustainability and multifunctionality in contemporary society encourages research to develop active materials that originate from renewable resources [1]. In this context, natural polymers have emerged as potential biopolymers for the synthesis of multifunctional materials owing to the abundance of hydroxyl groups present in their molecular structure, which provide significant opportunities for functionalization [2]. Cellulose, the main component of plant cell walls, is an intriguing biopolymer. It is a linear homopolysaccharide consisting of β-D-anhydroglucopyranose units that are connected by β(1→4) ether bonds (glycosidic links) and its chemical formula is $(C_6H_{10}O_5)n$ [3]. It can be obtained from origins, such as wood, plant cell walls, several bacteria strains, algae, and even tunicate marines, which are the only defined cellulose-producing animals [4, 5]. BC is a substance obtained from bacteria and is capable of being produced in a nearly pure form (up to 90%) without any other components, including hemicellulose and lignin. Its composed of glucose units with the same chemical structure as plant cellulose [6]. BC exhibits several distinctive qualities, including high water retention capacity, ultrafine network purity (high purity), degree of crystallinity, mechanical strength, degree of polymerization, formability, hydrophilicity, biocompatibility, flexibility, lack of toxicity, biodegradability, and useful mechanical properties (Young's modulus value, tensile strength, compressibility, and elongation) [7–10]. The functionalization of BC is a widely common challenge reported for application in different fields due to the inherent limitations of BC. To surmount this challenge, there have been numerous attempts to functionalize BC using either an in situ or ex situ approach with the aim of generating a functionalized polymeric composite with distinctive applications. Several studies have focused on the ex situ modification of BC for the purpose of advancing novel applications, like, Silver montmorillonite can be employed as an antimicrobial agent from the perspective of wound healing

✉ Ahmed K. Saleh
asrk_saleh@yahoo.com

[1] Cellulose and Paper Department, National Research Centre, 33 El Bohouth St., P.O. 12622, Dokki, Giza, Egypt

[2] Department of Chemistry, Faculty of Science, University of Tabuk, Tabuk, Saudi Arabia

[3] Department of Biochemistry, Faculty of Science, University of Tabuk, Tabuk, Saudi Arabia

Published online: 03 January 2024

treatment [11], silver sulfadiazine is employed in the context of diabetic wound healing [12], the utilization of extract of fruit peels for the purpose of antimicrobial applications and in the packaging of strawberries [13], additionally Poly(3,4 ethylenedioxythiophene)/Poly(styrenesulfonate) for optoelectronic applications [14]. Among them, nanomaterials are frequently used as novel antibacterial agents against infectious pathogens [15, 16]. Metal, metal oxide-NPs can inactivate pathogenic microbes by damaging the cell membrane, cell wall, electron transport chain, nucleic acids, proteins or enzymes [17, 18]. Metal oxide-NPs, specifically ZnO-NPs are repeatedly selected due to their nontoxic nature, biological attributes, and remarkable chemical stability. ZnO-NPs are widely recognized NPs that offer numerous therapeutic benefits, including antimicrobial (bacteria and fungi), immunomodulatory, antioxidant, and anticancer effects. Nevertheless, there have been multiple reports highlighting diverse forms of toxicities, such as hepatotoxicity, pulmonary toxicity, neurotoxicity, and mutagenicity associated with use of ZnO-NPs [19]. ZnO-NPs have been utilized in various commercial applications including industrial, medical and agricultural applications [20–22]. ZnO-NP plays a crucial role in numerous biomedical applications such as antimicrobial, anticancer, antineoplastic, wound healing, ultraviolet scattering, angiogenic, and antioxidant properties [23, 24]. The nate BC was modified with NPs for the development of antimicrobial agents like BC/ZnO-NPs, which exhibited 90, 87.4, 94.3, and 90.9% activity against *E. coli*, *P. aeruginosa*, *S. aureus*, and *Citrobacter freundii*, respectively, and the nanocomposite showed significant (66%) healing activity in treated animals [25], BC/Copper oxide-NPs nanohybrids exhibit that the antibacterial activity of ex situ synthesized nanohybrids against *S. aureus* and *E. coli* bacteria was greater than both in situ synthesized samples [26], BC/Carbon Quantum Dots-Titanium Dioxide-NPs have antibacterial properties against *S. aureus* [27], and the bionanocomposite of BC/Magnesium Oxide-NPs showed the highest antifungal activity and prevented the growth of the fungus *Aspergillus niger* by 85.03% [28]. As per current state of art today is that it is being develop scaffold materials based on the ex situ modification of BC with ZnO-NPs, and other published article related to functionalization of BC with ZnO-NPs for development of nanocomposite as a dressing system for burn wounds treatment [25]. The preparation of BC/ZnO-NPs nanocomposites were reported by in situ technique through the immersing of BC in zinc salt solution, followed by treating with NaOH solution and then dried through appropriate methods [29]. The current study aims to evaluate the BC network to support the immobilization of ZnO-NPs through ex situ technique. The novel aspect of this study was the modification of BC to enhance its medical applications, such as antimicrobial assessment. In this investigation, a BC/ZnO-NPs nanocomposite membrane was developed by reinforcing BC with ZnO-NPs. The pure BC and nanocomposite membranes obtained were analyzed by SEM, TEM, FT-IR, and XRD. The obtained membranes were evaluated as antimicrobial agents against four pathogenic microbes, and the results demonstrated that the BC/ZnO-NPs nanocomposite membrane successfully suppressed the growth of microorganisms.

2 Materials and methods

2.1 Production of BC hydrogel

2.1.1 Strain and standard inoculum

According to the previous investigation, *Lactiplantibacillus plantarum* AS.6 (*L. plantarum* AS.6) was identified as a strain that produce BC. This strain was obtained from decaying apples and has the accession number (MW857479.1) that was isolated from decaying apples [30]. For the preparation of standardized inoculum, a freshly and purely single colony of *L. plantarum* AS.6 was cultivated in the standard Hestrin and Schramm (HS) medium. The medium consisted of 20 g/L glucose, 5 g/L yeast extract, 5 g/L peptone, 2.7 g/L disodium hydrogen phosphate, 1.15 g/L citric acid, and 5 mL/L ethanol at pH 5.5. The cultivation was carried out at 30 °C for 48 h at 150 rpm [31].

2.1.2 Production and purification of BC hydrogel

In accordance with the findings presented in our prior investigation, after conventional and statistical optimization approaches, the final optimized medium was used for BC production by using the following optimal conditions: 15 g/L glucose, 13 g/L yeast extract, 1 g/L magnesium sulphate, 4 g/L potassium dihydrogen phosphate, and 7 mL/L ethanol [30], at pH 7.2. The media were sterilized at a temperature of 121 °C and a pressure of 15 psi for a duration of 20 min, and they were allowed to cool down to room temperature, and subsequently inoculated with 11% standard inoculum of *L. plantarum* and incubated at 30 °C, for 8 days of cultivation time under static conditions [30]. At the completion of the cultivation period, the BC pellicle observed at the air–liquid interface was gathered and repeatedly rinsed with distilled water in order to eliminate the excess medium ingredients. Following that, the BC hydrogel was treated with 0.5% sodium hydroxide at 90 °C for 30 min to kill the remnant *L. plantarum* AS.6 or other impurities embedded on the BC hydrogel, and washed with distilled water until it reached the point of a neutral pH value, after which a bright-white BC hydrogel was obtained. The purified BC hydrogel was kept in the refrigerator at 4 °C until used.

2.2 Ex situ *preparation of BC/ZnO-NPs nanocomposite membrane*

For the preparation of the BC/ZnO-NPs nanocomposite membrane, ZnO-NPs was used to modify the BC hydrogel by ex situ modification in accordance with the method of Khalid et al. [25], with slight changes as shown in Fig. 1. First, the purified BC hydrogel was cut into small fragments, each measuring 2 cm^2 in diameter and 3 mm in thickness. Each piece was subjected to compression through the utilization of filter paper, facilitating the expulsion of a significant portion of the water content. About 2% (v/v) of ZnO-NPs (Aldrich chemistry, ≤ 40 nm average particle size (APS), 20 wt.% in H_2O) was dispersed by using a very mild water bath sonication (720 W, 50/60 Hz, 230 V, Spain) at 50 °C for 30 min, and then homogenized by ultrasonication (750 wt, 20 KH, pulse 45, Amp 1) for 5 min under an ice-water bath to ensure the complete dispersion of ZnO-NPs. Small fragments of BC hydrogel (2 cm^2) were submerged in 100 mL of dispersed ZnO-NPs solution for 1 day at room temperature under shaking conditions (150 rpm) to assure the complete absorption of the dispersed ZnO-NPs on the BC hydrogel. The prepared nanocomposite hydrogel was immersed in distilled water for 10 s and treated with filter paper for the removal of extra-free water from the nanocomposite hydrogel. Finally, the obtained nanocomposite hydrogel was freeze-dried and stored at 4◦C for further use. The experiment was carried out in triplicate.

2.3 Microstructure characterization of BC and BC/ZnO-NPs nanocomposite membrane

2.3.1 SEM analysis

The BC and BC/ZnO-NPs nanocomposite membranes were analyzed through various instrumental techniques. The surface morphology of the obtained membrane was conducted using a Hitachi S-4800 SEM. The average diameter of the nanofiber was calculated from various SEM images using the angle tool of ImageJ with Java 1.8.0 software developed by the National Institute of Health (NIH), USA) [32].

2.3.2 TEM analysis

Ultra-high-resolution TEM (JEOL-JEM 2010, Japan) was utilized to investigate the internal composition structure of the BC/ZnO-NPs nanocomposite membrane.

2.3.3 FT-IR spectroscopy analysis

The FT-IR (model FT-IR-6100 type A) was employed to analyze the chemical functional groups found in both BC and BC/ZnO-NPs nanocomposite membranes. The measurement

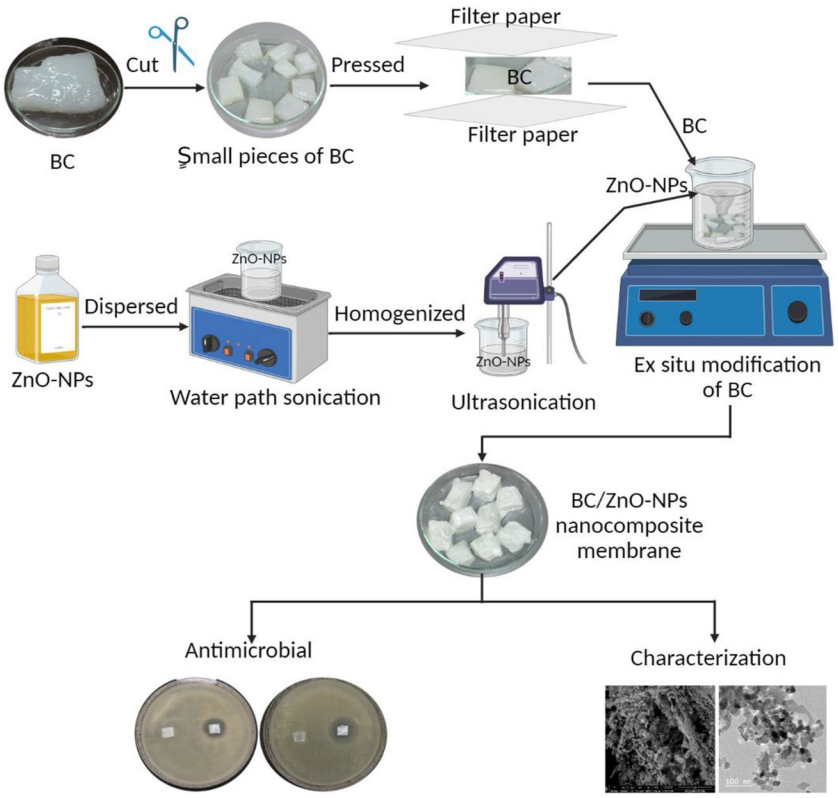

Fig. 1 Schematic illustrating the ex situ modification of BC hydrogel for the formation of a BC/ZnO-NPs nanocomposite membrane

of the spectra of each sample was conducted within a spectral range spanning from 500 to 4000 cm^{-1}.

2.3.4 XRD analysis

Analyzing the crystallinity of the acquired samples was performed using an X-ray diffractometer (XRD, Philips X' pert MPD, PANalytical, Netherlands) employing the CuKα line (λ = 1.540 Å) in the diffraction 2θ angular range 10–80°.

2.4 Antimicrobial activity

Mueller Hinton media comprising 0.15% starch, 1.75% acid hydrolysate of casein, and 0.2% beef extract was used as the growth medium for the microbial strains procured from the American Type Culture Collection (ATCC), including Gram-negative bacteria *Escherichia coli* ATCC 25922 (*E. coli*) and *Salmonella typhimurium* ATCC 14028 (*S. typhimurium*), Gram-positive bacteria *Streptococcus mutans* ATCC 25175 (*S. mutans*), and yeast *Candida albicans* ATCC 10231 (*C. albicans*). All the microorganisms employed in the study were cultivated for one day at 37°C, and incubated under agitated conditions at 200 rpm. The antimicrobial properties of BC and BC impregnated with ZnO-NPs (BC/ZnO-NPs) membranes were investigated qualitatively using the disc diffusion procedure, according to our previous study with some modifications [33]. Firstly, an amount of approximately 15 mL of sterilized Mueller Hinton media (20 g/L agar) was poured on the Petri dish and allowed to solidify. The microbial suspension (10^8 CFU/mL) which had a concentration or density approximately equal to 0.5 McFarland standards was evenly spread on the Petri dish along with a 10 mm disc of BC/ZnO-NPs. As a control, a sample without ZnO-NPs was used. The plates were first incubated at 4°C for 2 h to complete the diffusion of the tested sample and momentarily inhibit the model microbes. After that, they were cultivated at 37°C for 1 day. After the period of cultivation, the plates were estimated for their antimicrobial properties by measuring the diameter of the inhibition zone (including the membrane disc). The results represented are the average values of triplicate experiments. All membranes were sterilized for 30 min under UV light in order to ensure aseptic conditions.

3 Results and discussions

3.1 Microstructure characterization

3.1.1 SEM and TEM analysis

The first step in our research investigation involved examining the chemical composition and morphology of pure BC and BC that had been modified with ZnO-NPs. The SEM images of BC show a successful elimination of impurities along the BC network during treatment with 0.5 M NaOH. Furthermore, the nanofibers displayed an uneven distribution, which further confirmed the presence of porous areas within the membranes (Fig. 2A) in accordance with previous literature [34, 35]. In addition, the SEM images shown in Fig. 2B revealed that the average nanofiber diameter of the BC membrane obtained was measured to be 40.49 nm, as illustrated in fiber diameter measurements, which is in line with Zhang et al. and Almasi et al. [36, 37]. To investigate the formation of nanocomposite BC/ZnO-NPs, SEM images of the surface of the BC/ZnO-NPs nanocomposite membrane were taken. Inspection of Fig. 2 (C and D) reveals that the BC nanofibers were consistently covered by ZnO-NPs, showing that the ZnO-NPs regularly covered the BC nanofibers to form coating layers. The ZnO-NPs were able to permeate the BC pellicle individually without direct contact with the nanofibers through the diffusion method. There is no form of interaction observed between ZnO-NPs and BC fibers. Consequently, the NPs would physically deposit (e.g., driven by gravity) onto the BC nanofibers. The proposition was substantiated by the occurrence of random dispersion of the NPs. When the nanocomposite was established, the interior network and the exterior surface of the nanocomposites had ZnO-NPs. These results are in agreement with other reports by Khalid et al. [25]. TEM image of BC/ZnO-NPs nanocomposite membrane at high magnification showed the formation of ZnO-NPs with a size of 30 nm. These regular particles showed uniform size distribution.

3.1.2 FT-IR and XRD analysis

The chemical composition of the acquired samples, such as functional groups and molecular bonds, was determined by FT-IR spectroscopy. The FT-IR spectra of the BC sample derived from *L. plantarum* AS.6 were observed within the wavenumber range of 500 to 4000 cm^{-1} as depicted in Fig. 3A. A strong area of absorption in the BC spectrum at 3330.3 cm^{-1} corresponds to the intra-molecular hydrogen bond of the hydroxyl (OH) of cellulose type I, which aligns with [38, 39]. While the band at 2885 cm^{-1} was assigned to aliphatic C-H stretching vibration, the cellulose absorption spectrum includes a band at 1635.2 cm^{-1} which has been designated for the carboxyl (C = O) functional group. Bands were also detected at 1431.2 cm^{-1} signifying the bending of CH_2 bending; 1340.5 cm^{-1} (symmetric angular deformation of C H bonds), 1161.4 cm^{-1} indicating asymmetrical stretching of C–O–C, 1109.5 cm^{-1} and 1045.3 cm^{-1} (stretching of C–OH and C–C-OH bonds in secondary and primary alcohols). These findings are consistent with [30, 40]. Finally, the FT-IR result ultimately demonstrates the existence of a crystalline region and the exceptional purity of BC. The characteristic absorption bands for both BC and BC/ZnO

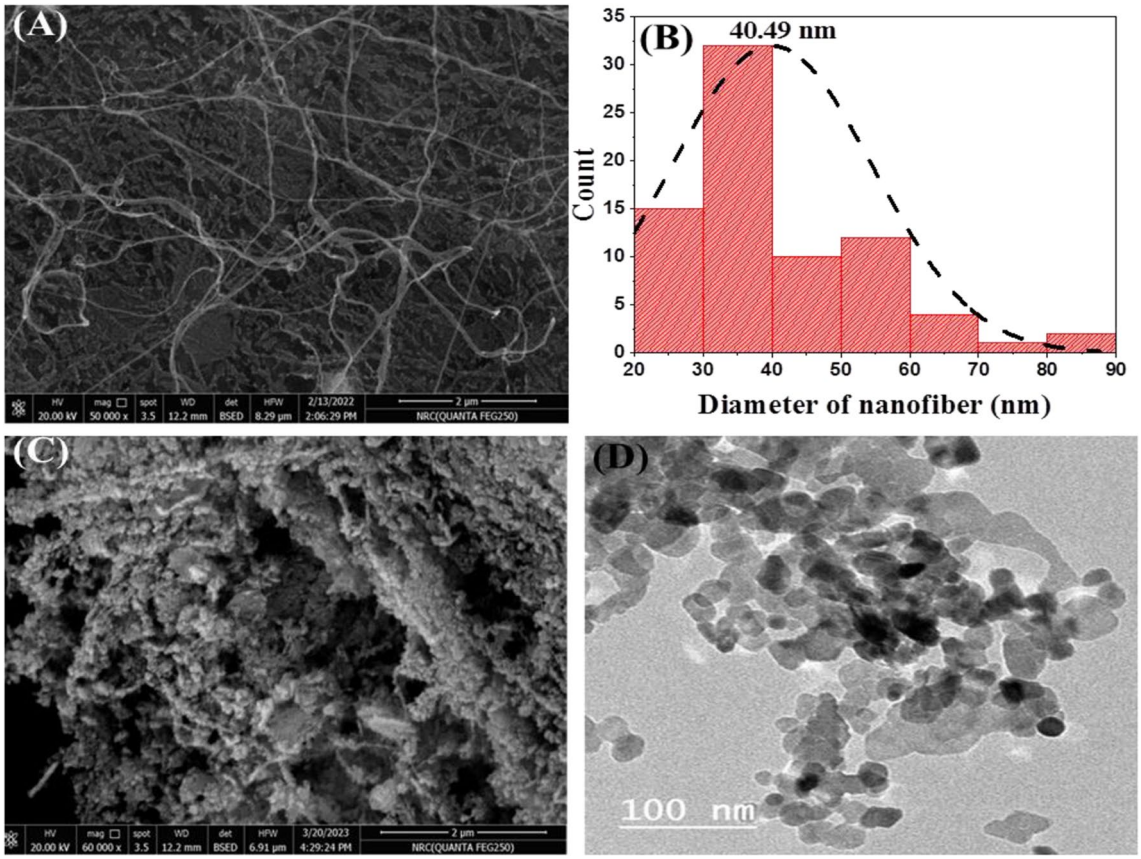

Fig. 2 **A** SEM image of pure BC, (**B**) Nanofiber diameter of BC, (**C**, and **D**) SEM and TEM images of BC/ZnO-NPs nanocomposite membrane, respectively

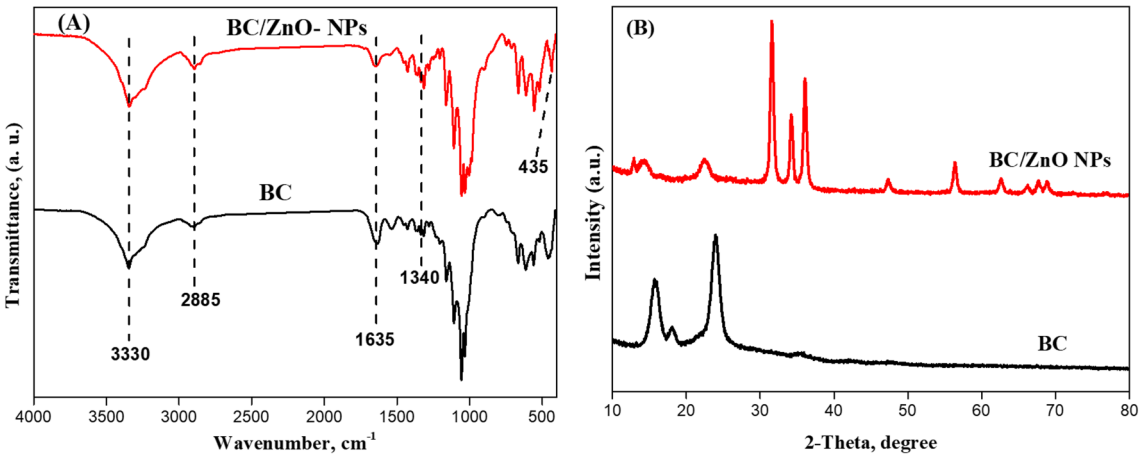

Fig. 3 FT-IR spectra (**A**) and XRD analysis (**B**) for pure BC and BC/ZnO-NPs nanocomposite membrane

nanocomposite were presented in the "fingerprint" region (400–1650 cm^{-1}). Some apparent changes appeared in the FT-IR spectrum of the BC/ZnO nanocomposite compared to pure BC. A new peak at 435 cm^{-1} assigned to the stretching mode of the Zn–O bond was recorded for the obtained BC/ZnO-NPs nanocomposite membrane [25]. The Zn–O vibrations were not sharp in the prepared composite due to the low ZnO content which was reported in previous study [41]. XRD was employed to reveal the crystal structure of the materials that were obtained. In Fig. 3B, XRD patterns of pure BC and BC/ZnO nanocomposite membranes are displayed. Both BC and BC/ZnO-NPs exhibit two strong,

wide peaks at 16.3 and 22.2°, as well as a less intense and sharp reflection at 34.4°. These signals correspond to the characteristic 110, 200, and 004 planes assigned to the typical cellulose-I structure. Additional peaks attributed to the presence of the ZnO-NPs were identified in the pattern of BC/ZnO-NPs. The high intensity may be attributed to the abundant presence of NPs covering the surface of BC. Several sharp and intense Bragg reflections were detected at 31.56°, 34.22°, 36.11°, 47.35°, 56.43°, 62.63°, 67.72°, and 68.92°. These reflections well corresponded with the described peak positions for bulk ZnO (in accordance with standard PDF card no. 01–079-0207) demonstrating the existence of a wurtzite hexagonal crystal structure of ZnO. Moreover, these results indicate that ZnO was well crystallized in the composite. Moreover, the diffraction peaks of cellulose in the composite were much weaker. This might be affected by ZnO-NPs which cover the cellulose surface, making hard to collect the diffraction data of BC through the XRD study [42].

3.2 Antimicrobial assessment

The disc diffusion technique was used to investigate the antimicrobial activities of BC and BC/ZnO-NPs nanocomposite membranes against pathogenic strains. According to the results illustrated in Table 1 and Fig. 4, the data indicated a significant antimicrobial activity against all employing pathogens through the BC/ZnO-NPs nanocomposite membrane, which aligns with [25, 43, 44]. The BC/ZnO-NPs nanocomposite membrane showed higher antimicrobial activity against *S. typhimurium* (21 ± 1.21 mm), with no significant effects against *E. coli* (18 ± 1.15 mm) or *S. mutans* (19 ± 1.19 mm), while the lowest antimicrobial activity was shown against *C. albicans* (14 ± 1.06 mm). In contrast, the BC membrane free from NPs showed no antimicrobial activity against any of the tested microbes, which is supported by existing literatures [13, 33, 45]. We can conclude that the antimicrobial activity existed only due to ZnO-NPs impregnated inside the BC membrane and was not attributed to individual BC. To overcome this problem, the BC membrane was loaded or fabricated with NPs for the development of an antimicrobial membrane, for example, ZnO-NPs [46], Ag-NPs [47], CuO-NPs [33, 48], and MgO-NPs [28]. The antimicrobial efficacy of BC/ZnO-NPs nanocomposite membrane has been extensively documented; however, the primary mode of action has yet to be completely understood. The mechanism of action of the ZnO-NPs is based on their morphology, concentration, and composition [49]. The primary mechanisms of the antimicrobial properties of ZnO-NPs are the generation of reactive oxygen species (ROS), the release of Zn^{+2}, internalization of ZnO-NPs into microbes, and electrostatic interactions. These mechanisms modify the external membrane, disrupt the cell wall, induce protein denaturation, oxidize the lipid membrane, and cause oxidative DNA damage in microorganisms [50–52]. Other metal oxide-NPs, specially CuO-NPs based on their binding with the lipid layer of the bacterial cell membrane, which interferes with membrane permeability and nutrient uptake, were proposed to elaborate such activity [53], while the antibacterial activity of MgO-NPs is attributed to the production of ROS, which induce lipid peroxidation in bacteria [54], while the antimicrobial activity of Ag-NPs is based on the release of Ag^{+1} ions into the solution and then bind the bacterial membrane and proteins, causing cell lysis. The Ag^{+1} ions can originate from the solution but may also be transferred

Table 1 Antimicrobial activity of BC and BC/ZnO-NPs nanocomposite membranes against four pathogenic microbes

Model of microbes	Diameters of inhibition zone (mm)	
	BC	BC/ZnO-NPs
E. coli	0.0 ± 0.0	18 ± 1.15
S. typhimurium	0.0 ± 0.0	21 ± 1.21
S. mutans	0.0 ± 0.0	19 ± 1.19
C. albicans	0.0 ± 0.0	14 ± 1.06

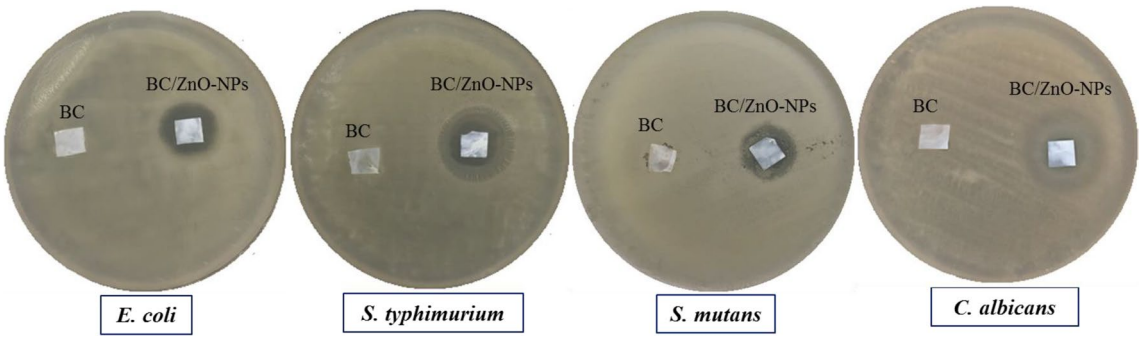

Fig. 4 Disc diffusion method for antimicrobial activity expressed as halo zones of BC and BC/ZnO-NPs nanocomposite membranes against four pathogenic microbes

Table 2 Comparison of BC impregnated with NPs with previously reported composite membrane

Composite membrane	Model of microbes	Inhibition zoon diameter (mm)	Reference
BC/ZnO-NPs	*E. coli*	18 ± 1.15	Current study
	S. typhimurium	21 ± 1.21	
	S. mutans	19 ± 1.19	
	C. albicans	14 ± 1.06	
BC/ZnO-NPs	*E. coli*	27 ± 0	[25]
	P. aeruginosa	25 ± 1	
	S. aureus	28.6 ± 1.15	
	Citrobacter freundii	26 ± 0	
BC/Ag-NPs	*E. coli*	2	[56]
	S. aureus	9	
BC/Quantum Dots- TiO_2-NPs	*E. coli*	ND	[27]
	S. aureus	13	
BC/CuO-NPs	*S. aureus*	30.9	[48]
	Salmonella enterica	13.2	
	C. albicans	25.9	
BC/MgO-NPs	*E. coli*	18.32 ± 1.19	[57]
	S. aureus	25.11 ± 3.02	
BC/PVA/chitosan-NPs	*E. coli*	10.00 ± 0	[58]
	S. aureus	10.33 ± 1.55	
BC/Cu-SiO_2-NPs	*E. coli*	3.0	[59]
	S. aureus	4.0	
BC/graphene oxide/Ag-NPs	*E. coli*	6.3	[60]
BC/gelatin/Selenium-NPs	*E. coli*	ND	[61]
	S. aureus	22	
BC/ TiO_2-NPs	*E. coli*	ND	[62]

ND not detected

directly from the surface-exposed Ag^{+1} ions to the bacteria without being dissolved in the medium [55]. We can summarize the BC functionalized with NPs as having antimicrobial activity, as presented in Table 2.

4 Conclusion

BC was prepared and decorated with ZnO-NPs for preparing nanocomosite membranes as antimicrobial agents for wound healing applications. The formed nanocomposite membranes were characterized and evaluated by chemical analysis and biological assessments. The FT-IR and XRD analayses proved the decoration process, while SEM and TEM results exhibited the formation of BC/ZnO-NPs nanocomposite membrane with a homogenous distribution of the ZnO-NPs which are regularly covered by the BC nanofibers to form coating layers. The BC/ZnO-NPs nanocomposite exhibits high antibacterial properties, as displayed by the formation of the inhibition zone for *S. typhimurium* (21 mm), *E. coli* (18 mm), and *S. mutans* (19 mm), while the lowest antimicrobial activity was shown against *C. albicans* (14 mm). The antimicrobial activity of the nanocomposite is related to the presence of ZnO-NPs. Therefore, BC/ZnO-NPs nanocomposite membranes have significant potential for application as an antimicrobial biomembrane for wound healing activity.

Author contribution **Ahmed K. Saleh:** Conceptualization, Formal analysis, Investigation, Methodology, Writing—review & editing Data curation. **Ali Hamzah Alessa:** Writing—review & editing. **Awatif M. E. Omran:** Writing—review & editing.

Funding Open access funding provided by The Science, Technology & Innovation Funding Authority (STDF) in cooperation with The Egyptian Knowledge Bank (EKB).

Data availability All data generated or analyzed during this study are included in this published article.

Declarations

Ethics approval Not applicable.

Competing interests The authors declare no competing interests.

References

1. Salama A, Hesemann P (2018) New N-guanidinium chitosan/silica ionic microhybrids as efficient adsorbent for dye removal from waste water. Int J Biol Macromol 111:762–768
2. Wieszczycka K, Staszak K, Woźniak-Budych MJ, Litowczenko J, Maciejewska BM, Jurga S (2021) Surface functionalization–The way for advanced applications of smart materials. Coord Chem Rev 436:213846
3. Wohlhauser S, Delepierre G, Labet M, Gl Morandi, Thielemans W, Weder C, Zoppe JO (2018) Grafting polymers from cellulose nanocrystals: Synthesis, properties, and applications. Macromolecules 51(16):6157–6189
4. Klemm D, Heublein B, Fink HP, Bohn A (2005) Cellulose: fascinating biopolymer and sustainable raw material. Angew Chem Int Ed 44(22):3358–3393
5. Lynd LR, Weimer PJ, Van Zyl WH, Pretorius IS (2002) Microbial cellulose utilization: fundamentals and biotechnology. Microbiol Mol Biol Rev 66(3):506–577
6. Huang CZ, Yang J, Nie Y, Chen C, Sun D (2014) Recent advances in bacterial cellulose. Cellulose 21(1):1–30
7. Rajwade J, Paknikar K, Kumbhar J (2015) Applications of bacterial cellulose and its composites in biomedicine. Appl Microbiol Biotechnol 99:2491–2511
8. Vasconcelos NF, Feitosa JPA, da Gama FMP, Morais JPS, Andrade FK, de Souza MdSM, de Freitas Rosa M (2017) Bacterial cellulose nanocrystals produced under different hydrolysis conditions: Properties and morphological features. Carbohydr Polym 155:425–431
9. Costa A, Rocha MAV, Sarubbo L (2017) Bacterial cellulose: an ecofriendly biotextile. Int J Text Fash Technol 7:11–26
10. Wang J, Tavakoli J, Tang Y (2019) Bacterial cellulose production, properties and applications with different culture methods–A review. Carbohydr Polym 219:63–76
11. Horue M, Cacicedo ML, Fernandez MA, Rodenak-Kladniew B, Sánchez RMT, Castro GR (2020) Antimicrobial activities of bacterial cellulose–Silver montmorillonite nanocomposites for wound healing. Mater Sci Eng C 116:111152
12. Aris FAF, Fauzi FNAM, Tong WY, Abdullah SSS (2019) Interaction of silver sulfadiazine wıth bacterial cellulose via ex-situ modification method as an alternative diabetic wound healing. Biocatal Agric Biotechnol 21:101332
13. El-Gendi H, Salama A, El-Fakharany EM, Saleh AK (2023) Optimization of bacterial cellulose production from prickly pear peels and its ex situ impregnation with fruit byproducts for antimicrobial and strawberry packaging applications. Carbohydr Polym 302:120383
14. Khan S, Ul-Islam M, Khattak WA, Ullah MW, Park JK (2015) Bacterial cellulose–poly (3, 4-ethylenedioxythiophene)–poly (styrenesulfonate) composites for optoelectronic applications. Carbohydr Polym 127:86–93
15. Jayarajan D, Sagayaraj R, Silvan S, Sebastian S, Nithya R, Sujeetha S (2023) Green synthesis, Structural and Magnetic Properties of Mg0. 5Zn0. 5Fe2O4 Ferrite Nanoparticles by the Coprecipitation Method: Averrhoa bilimbi fruit. Chem Africa 6:1875–185
16. AK Saleh, AS Shaban, MA Diab, D Debarnot, AS Elzaref (2023) Green synthesis and characterization of aluminum oxide nanoparticles using Phoenix dactylifera seed extract along with antimicrobial activity, phytotoxicity, and cytological effects on Vicia faba seeds, Biomass Convers. Biorefin https://doi.org/10.1007/s13399-023-04800-x
17. Alavi M, Hamblin MR, Martinez F, Kennedy JF, Khan H (2022) Synergistic combinations of metal, metal oxide, or metalloid nanoparticles plus antibiotics against resistant and non-resistant bacteria. Micro Nano Bio Aspects 1(1):1–9
18. Alavi M, Kowalski R, Capasso R, Melo Coutinho HD, Alencar De Menezes IR (2022) Various novel strategies for functionalization of gold and silver nanoparticles to hinder drug-resistant bacteria and cancer cells. Micro Nano Bio Aspects 1(1):38–48
19. Keerthana S, Kumar A (2020) Potential risks and benefits of zinc oxide nanoparticles: a systematic review. Crit Rev Toxicol 50(1):47–71
20. Shaban AS, Owda ME, Basuoni MM, Mousa MA, Radwan AA, Saleh AK (2022) Punica granatum peel extract mediated green synthesis of zinc oxide nanoparticles: structure and evaluation of their biological applications, Biomass Convers. Biorefin. https://doi.org/10.1007/s13399-022-03185-7
21. Vijayakumar S, Nilavukkarasi M, Vidhya E, Punitha V, Prathipkumar S (2023) Biogenesis of heneicosane mediated ZnO nanoparticles: characterization and biological efficiency. Chemistry Africa 6(1):551–557
22. Adegoke HI, Gbenga AA (2023) Bio-Assisted synthesis of zinc oxide nanoparticles from mimosa pudica aqueous leave extract: structure and antibacterial activity. Chemistry Africa 6:1283–1296
23. Cruz DM, Mostafavi E, Vernet-Crua A, Barabadi H, Shah V, Cholula-Díaz JL, Guisbiers G, Webster TJ (2020) Green nanotechnology-based zinc oxide (ZnO) nanomaterials for biomedical applications: a review. J Phys Mater 3(3):034005
24. Babayevska N, Przysiecka Ł, Iatsunskyi I, Nowaczyk G, Jarek M, Janiszewska E, Jurga S (2022) ZnO size and shape effect on antibacterial activity and cytotoxicity profile. Sci Rep 12(1):8148
25. Khalid A, Khan R, Ul-Islam M, Khan T, Wahid F (2017) Bacterial cellulose-zinc oxide nanocomposites as a novel dressing system for burn wounds. Carbohydr Polym 164:214–221
26. Almasi H, Mehryar L, Ghadertaj A (2019) Characterization of CuO-bacterial cellulose nanohybrids fabricated by in-situ and ex-situ impregnation methods. Carbohydr Polym 222:114995
27. Malmir S, Karbalaei A, Pourmadadi M, Hamedi J, Yazdian F, Navaee M (2020) Antibacterial properties of a bacterial cellulose CQD-TiO2 nanocomposite. Carbohydr Polym 234:115835
28. Safaei M, Taran M (2022) Preparation of bacterial cellulose fungicide nanocomposite incorporated with MgO nanoparticles. J Polym Environ 30:2066–2076
29. Wahid F, Duan Y-X, Hu X-H, Chu L-Q, Jia S-R, Cui J-D, Zhong C (2019) A facile construction of bacterial cellulose/ZnO nanocomposite films and their photocatalytic and antibacterial properties. Int J Biol Macromol 132:692–700
30. Saleh AK, El-Gendi H, Soliman NA, El-Zawawy WK, Abdel-Fattah YR (2022) Bioprocess development for bacterial cellulose biosynthesis by novel Lactiplantibacillus plantarum isolate along with characterization and antimicrobial assessment of fabricated membrane. Sci Rep 12(1):2181
31. Hestrin S, Schramm M (1954) Synthesis of cellulose by Acetobacter xylinum .2. Preparation of freeze-dried cells capable of polymerizing glucose to cellulose. Biochem J 58(2):345
32. Wang L, Mao L, Qi F, Li X, Ullah MW, Zhao M, Shi Z, Yang G (2021) Synergistic effect of highly aligned bacterial cellulose/gelatin membranes and electrical stimulation on directional cell migration for accelerated wound healing. Chem Eng J 424:130563
33. Saleh AK, El-Gendi H, El-Fakharany EM, Owda ME, Awad MA, Kamoun EA (2022) Exploitation of cantaloupe peels for bacterial cellulose production and functionalization with green synthesized Copper oxide nanoparticles for diverse biological applications. Sci Rep 12(1):19241
34. Mocanu A, Isopencu G, Busuioc C, Popa O-M, Dietrich P, Socaciu-Siebert L (2019) Bacterial cellulose films with ZnO

nanoparticles and propolis extracts: Synergistic antimicrobial effect. Sci Rep 9(1):17687
35. Retegi A, Gabilondo N, Peña C, Zuluaga R, Castro C, Gañán P, de La Caba K, Mondragon I (2010) Bacterial cellulose films with controlled microstructure–mechanical property relationships. Cellulose 17:661–669
36. Zhang T, Wang W, Zhang D, Zhang X, Ma Y, Zhou Y, Qi L (2010) Biotemplated synthesis of gold nanoparticle–bacteria cellulose nanofiber nanocomposites and their application in biosensing. Adv Funct Mater 20(7):1152–1160
37. Almasi H, Jafarzadeh P, Mehryar L (2018) Fabrication of novel nanohybrids by impregnation of CuO nanoparticles into bacterial cellulose and chitosan nanofibers: Characterization, antimicrobial and release properties. Carbohydr Polym 186:273–281
38. Rusdi RAA, Halim NA, Nurazzi MN, Abidin ZHZ, Abdullah N, CheRos F, Ahmad N, Azmi AFM (2022) Pre-treatment effect on the structure of bacterial cellulose from Nata de Coco (Acetobacter xylinum). Polimery 67:3
39. Jin YH, Lee T, Kim JR, Choi Y-E, Park C (2019) Improved production of bacterial cellulose from waste glycerol through investigation of inhibitory effects of crude glycerol-derived compounds by Gluconacetobacter xylinus. J Ind Eng Chem 75:158–163
40 Saleh AK, Soliman NA, Farrag AA, Ibrahim MM, El-Shinnawy NA, Abdel-Fattah YR (2020) Statistical optimization and characterization of a biocellulose produced by local Egyptian isolate Komagataeibacter hansenii AS. 5. Int J Biol Macromol 144:198–207
41. Fu F, Li L, Liu L, Cai J, Zhang Y, Zhou J, Zhang L (2015) Construction of cellulose based ZnO nanocomposite films with antibacterial properties through one-step coagulation. ACS Appl Mater Interfaces 7(4):2597–2606
42. Zhao S-W, Zheng M, Zou X-H, Guo Y, Pan Q-J (2017) Self-assembly of hierarchically structured cellulose@ ZnO composite in solid–liquid homogeneous phase: synthesis DFT calculations, and enhanced antibacterial activities. ACS Sustain Chem Eng 5(8):6585–6596
43. Kai J, Xuesong Z (2020) Preparation, characterization, and cytotoxicity evaluation of zinc oxide–bacterial cellulose–chitosan hydrogels for antibacterial dressing. Macromol Chem Phys 221(21):2000257
44. Jebel FS, Almasi H (2016) Morphological, physical, antimicrobial and release properties of ZnO nanoparticles-loaded bacterial cellulose films. Carbohydr Polym 149:8–19
45 Shaaban MT, Zayed M, Salama HS (2023) Antibacterial Potential of Bacterial Cellulose Impregnated with Green Synthesized Silver Nanoparticle Against S. aureus and P. aeruginosa. Curr Microbiol 80(2):75
46. Heydari S, Asefnejad A, Nemati NH, Goodarzi V, Vaziri A (2022) Fabrication of multicomponent cellulose/polypyrrole composed with zinc oxide nanoparticles for improving mechanical and biological properties. React Funct Polym 170:105126
47. Anwar Y, Ul-Islam M, Ali HSM, Ullah I, Khalil A, Kamal T (2022) Silver impregnated bacterial cellulose-chitosan composite hydrogels for antibacterial and catalytic applications. J Market Res 18:2037–2047
48. Araújo IM, Silva RR, Pacheco G, Lustri WR, Tercjak A, Gutierrez J, Júnior JR, Azevedo FH, Figuêredo GS, Vega ML (2018) Hydrothermal synthesis of bacterial cellulose–copper oxide nanocomposites and evaluation of their antimicrobial activity. Carbohydr Polym 179:341–349
49. Mendes CR, Dilarri G, Forsan CF, Sapata VdMR, Lopes PRM, de Moraes PB, Montagnolli RN, Ferreira H, Bidoia ED (2022) Antibacterial action and target mechanisms of zinc oxide nanoparticles against bacterial pathogens. Sci Rep 12(1):2658
50. Sirelkhatim A, Mahmud S, Seeni A, Kaus NHM, Ann LC, Bakhori SKM, Hasan H, Mohamad D (2015) Review on zinc oxide nanoparticles: antibacterial activity and toxicity mechanism. Nano-micro letters 7:219–242
51. da Silva BL, Abuçafy MP, Berbel Manaia E, Oshiro Junior JA, Chiari-Andréo BG, Pietro RCR, Chiavacci LA (2019) Relationship between structure and antimicrobial activity of zinc oxide nanoparticles: An overview. Int J Nanomed 14:9395–9410
52. Zhu X, Wang J, Cai L, Wu Y, Ji M, Jiang H, Chen J (2022) Dissection of the antibacterial mechanism of zinc oxide nanoparticles with manipulable nanoscale morphologies. J Hazard Mater 430:128436
53. Errokh A, Ferraria A, Conceição D, Ferreira LV, Do Rego AB, Vilar MR, Boufi S (2016) Controlled growth of Cu2O nanoparticles bound to cotton fibres. Carbohydr Polym 141:229–237
54. Tang Z-X, Lv B-F (2014) MgO nanoparticles as antibacterial agent: preparation and activity. Braz J Chem Eng 31:591–601
55. Knetsch ML, Koole LH (2011) New strategies in the development of antimicrobial coatings: the example of increasing usage of silver and silver nanoparticles. Polymers 3(1):340–366
56. Yang G, Xie J, Hong F, Cao Z, Yang X (2012) Antimicrobial activity of silver nanoparticle impregnated bacterial cellulose membrane: effect of fermentation carbon sources of bacterial cellulose. Carbohydr Polym 87(1):839–845
57. Mirtalebi SS, Almasi H, Khaledabad MA (2019) Physical, morphological, antimicrobial and release properties of novel MgO-bacterial cellulose nanohybrids prepared by in-situ and ex-situ methods. Int J Biol Macromol 128:848–857
58. Ju S, Zhang F, Duan J, Jiang J (2020) Characterization of bacterial cellulose composite films incorporated with bulk chitosan and chitosan nanoparticles: A comparative study. Carbohydr Polym 237:116167
59. Ma B, Huang Y, Zhu C, Chen C, Chen X, Fan M, Sun D (2016) Novel Cu@ SiO2/bacterial cellulose nanofibers: Preparation and excellent performance in antibacterial activity. Mater Sci Eng C 62:656–661
60. Zhang L, Yu Y, Zheng S, Zhong L, Xue J (2021) Preparation and properties of conductive bacterial cellulose-based graphene oxide-silver nanoparticles antibacterial dressing. Carbohydr Polym 257:117671
61. Mao L, Wang L, Zhang M, Ullah MW, Liu L, Zhao W, Li Y, Ahmed AAQ, Cheng H, Shi Z (2021) In situ synthesized selenium nanoparticles-decorated bacterial cellulose/gelatin hydrogel with enhanced antibacterial, antioxidant, and anti-inflammatory capabilities for facilitating skin wound healing. Adv Healthcare Mater 10(14):2100402
62. Khan S, Ul-Islam M, Khattak WA, Ullah MW, Park JK (2015) Bacterial cellulose-titanium dioxide nanocomposites: nanostructural characteristics, antibacterial mechanism, and biocompatibility. Cellulose 22:565–579